Report

The GTPase Regulatory Proteins Pix and Git Control Tissue Growth via the Hippo Pathway

Lucas G. Dent,[1,3] Carole L.C. Poon,[1,2] Xiaomeng Zhang,[1,2,3] Joffrey L. Degoutin,[1,2] Marla Tipping,[4] Alexey Veraksa,[5] and Kieran F. Harvey[1,2,3,*]

[1]Cell Growth and Proliferation Laboratory, Peter MacCallum Cancer Centre, 7 St Andrews Place, East Melbourne, VIC 3002, Australia
[2]Sir Peter MacCallum Department of Oncology, University of Melbourne, Parkville, VIC 3010, Australia
[3]Department of Pathology, University of Melbourne, Parkville, VIC 3010, Australia
[4]Department of Biology, Providence College, Providence, RI 02918, USA
[5]Department of Biology, University of Massachusetts Boston, Boston, MA 02125, USA

Summary

The Salvador-Warts-Hippo (Hippo) pathway is a conserved regulator of organ size and is deregulated in human cancers [1]. In epithelial tissues, the Hippo pathway is regulated by fundamental cell biological properties, such as polarity and adhesion, and coordinates these with tissue growth [2–4]. Despite its importance in disease, development, and regeneration, the complete set of proteins that regulate Hippo signaling remain undefined. To address this, we used proteomics to identify proteins that bind to the Hippo (Hpo) kinase. Prominent among these were PAK-interacting exchange factor (known as Pix or RtGEF) and G-protein-coupled receptor kinase-interacting protein (Git). Pix is a conserved Rho-type guanine nucleotide exchange factor (Rho-GEF) homologous to Beta-PIX and Alpha-PIX in mammals. Git is the single *Drosophila melanogaster* homolog of the mammalian GIT1 and GIT2 proteins, which were originally identified in the search for molecules that interact with G-protein-coupled receptor kinases [5]. Pix and Git form an oligomeric scaffold to facilitate sterile 20-like kinase activation and have also been linked to GTPase regulation [5–8]. We show that Pix and Git regulate Hippo-pathway-dependent tissue growth in *D. melanogaster* and that they do this in parallel to the known upstream regulator Fat cadherin. Pix and Git influence activity of the Hpo kinase by acting as a scaffold complex, rather than enzymes, and promote Hpo dimerization and autophosphorylation of Hpo's activation loop. Therefore, we provide important new insights into an ancient signaling network that controls the growth of metazoan tissues.

Results and Discussion

Pix and Git Physically and Genetically Interact with Hippo

The Hippo pathway regulates tissue growth by controlling the activation of a core kinase cassette, consisting of the kinases Hippo (Hpo) and Warts (Wts), and their respective cofactors Salvador (Sav) and Mob as tumor suppressor (Mats).

Activation of this cassette results in the phosphorylation and inactivation of the transcriptional activator Yorkie (Yki). Hpo is recognized as the most upstream kinase in the Hippo pathway core kinase cassette [9–12]. Multiple proteins regulate its activity, including Tao-1 [13, 14], RASSF [15], and the STRIPAK phosphatase complex [16]. To identify additional regulators of Hpo, we used affinity purification of Hpo tagged at both the N and C termini in *Drosophila melanogaster* S2 cells, followed by mass spectrometry [17]. We recovered several known Hippo pathway proteins, including Rassf, Sav, and Yki. Among the most abundant Hpo-interacting proteins were PAK-interacting exchange factor (Pix) and G-protein-coupled receptor kinase-interacting protein (Git); Pix was identified with five peptides and a SAINT probability of 0.999, whereas Git was represented with 15 peptides and a maximal SAINT probability of 1 (Table S1 available online) [18]. Furthermore, in an independent study, both Pix and Git were recovered as Hpo-binding proteins [16]. To confirm these results, we performed coimmunoprecipitation experiments in S2 cells, and we found that Hpo formed a physical complex with both Pix and Git (Figures 1A and S1). We also performed coimmunoprecipitation experiments in *D. melanogaster* wing imaginal discs and demonstrated that Pix and Git physically interact in this tissue (Figure 1B).

Pix Regulates Hippo Pathway Activity

To investigate a role for Pix in mediating control of organ size by the Hippo pathway, we performed a number of experiments. Initially, we depleted Pix using RNAi in a sensitized Hippo pathway background (*GMR>Yki*) that we have used previously to identify novel Hippo pathway proteins [13, 19]. The *GMR>Yki* strain has eye specific Yki overexpression, which results in subtle eye overgrowth and an increase in interommatidial cells [13]. Pix depletion in *GMR>Yki* eyes gave rise to an increase in adult eye size, with folding and convolution of the eye, consistent with enhanced Yki activity (Figures 1C–1D′). Indeed, RNAi-mediated depletion of the key Yki transcription factor Scalloped (Sd) completely suppressed the ability of Yki overexpression and Pix-RNAi to enhance eye size (Figures 1E and 1E′). We also found in larval wing imaginal discs that Pix depletion caused an increase in both *ex-lacZ* and *ban-lacZ*, well-established reporters of Yki activity [20–22] (Figures 1F, 1F′, S1E, and S1E′). The observed increase in *ex-lacZ* was dependent on Yki, as codepletion of Pix and Yki suppressed this increase (Figures S1D and S1D′). Collectively, these in vivo data provide evidence that Pix regulates Hippo-pathway-dependent tissue growth.

Pix and Git Limit Tissue Growth in Parallel to Fat Cadherin

To assess the role of Pix and Git in tissue growth further, we assessed animals that were mutant for the genes encoding these proteins. Both *pix* and *git* mutant animals were semiviable; adults that emerged displayed a crumpled wing phenotype, which precluded measurement of size (data not shown). No obvious overgrowth was observed in other adult tissues, such as the eye. A common theme with upstream regulators of the Hippo pathway is that they operate in a redundant

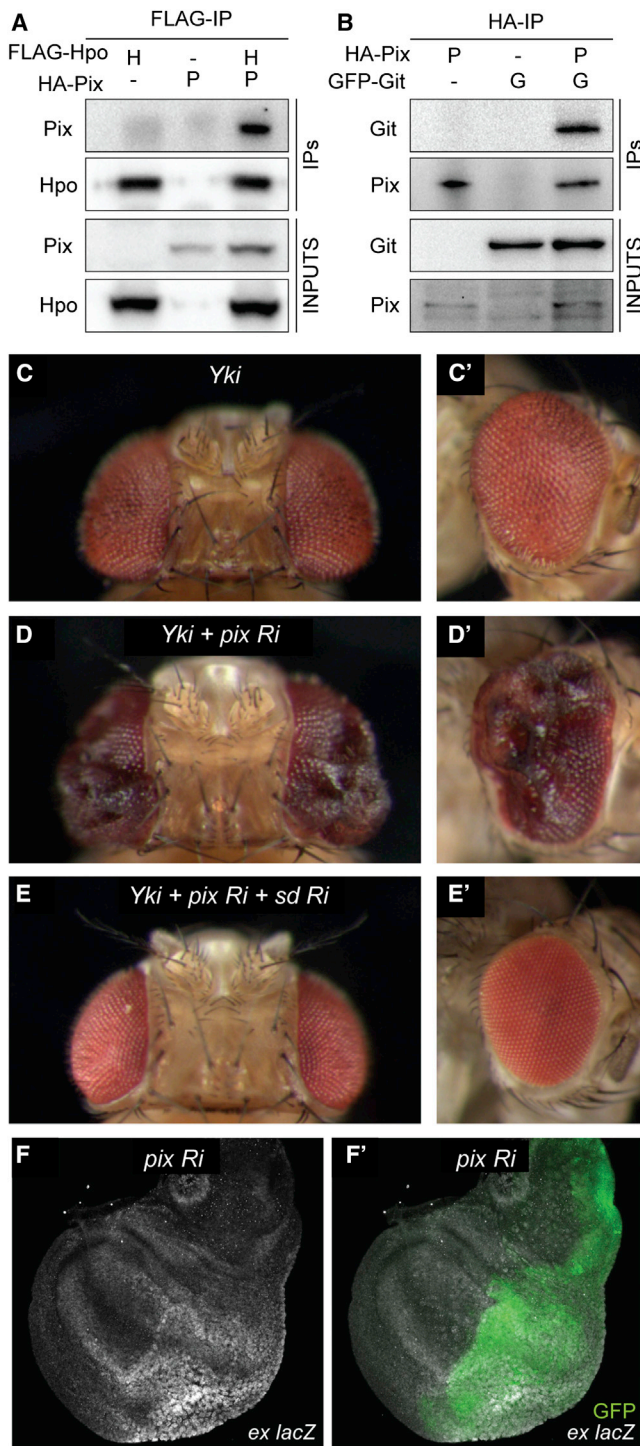*Correspondence: kieran.harvey@petermac.org

Figure 1. Pix and Git Physically Interact with Hippo and Regulate Hippo Pathway Activity

(A and B) For coimmunoprecipitation experiments, protein lysates from S2 cells transfected with the indicated plasmids (A) or wing imaginal discs expressing the indicated transgenes (B) were incubated with anti-Flag or anti-hemagglutinin (anti-HA) antibodies, respectively. Western blot analysis was performed using anti-Flag, anti-HA, and anti-GFP antibodies to reveal Hpo, Pix, and Git, respectively.

(C–E′) Adult female *D. melanogaster* eyes, with dorsal views in (C), (D), and (E) and lateral views in (C′), (D′), and (E′). Eyes express *UAS-Yki-S168A-YFP* under the control of *GMR-Gal4* alone (C and C′), with *UAS-Pix RNAi* (D and D′), or with *UAS-Pix RNAi* and *UAS-Sd RNAi* (E and E′).

fashion [23]. Double-mutant analysis has revealed that several upstream Hippo pathway proteins can compensate for each other. For example the loss of either *merlin* (*mer*), *fat*, *ex*, or *kibra* alone gives subtle overgrowth phenotypes whereas tissues that are double mutant for these sets of genes show very strong overgrowth [20, 24–27]. Therefore, we reasoned that Pix and Git's ability to regulate Hippo-pathway-dependent tissue growth might be masked by functional redundancy. To test this idea, we made a series of double- or triple-mutant animals with either *fat* or *ex* (*pix, fat*; *pix, fat, ex*; and *fat, git*), as Fat and Ex are well-defined upstream Hippo pathway proteins [20, 28–31] and are thought to operate, at least in part, in separate branches of the Hippo pathway [23].

Initially, we used the *eyeless-FLP* system to create clones of tissue lacking *pix*, *fat*, or both genes in the eye and head capsule. Adult heads containing *pix* mutant clones displayed no obvious overgrowth, whereas those with loss of *fat* showed slightly larger eyes and overgrowth in the head capsule compared to controls (Figures 2A–2C). Compound mutation of both *fat* and *pix* or *fat* and *git* genes caused substantial overgrowth, particularly in the ptilinum compared to loss of each gene in isolation (Figures 2D and S2). These phenotypes were reminiscent of eye and head tissue that also lack both *fat* and *ex* compared to tissue lacking only one of these genes (Figures 2C, 2E, and 2F). Interestingly, tissue mutant for *fat*, *pix*, and *ex* showed further overgrowth (Figure 2G). The enhanced tissue overgrowth in *fat, pix* and *fat, ex, pix* mutants was also manifest in reduced adult survival. Animals with *fat, pix* double-mutant head tissue were less viable than animals with *fat* mutant head tissue alone, and animals with *fat, ex, pix* head tissue were 100% lethal (Figure 2H).

Animals that were homozygous mutant for both *fat* and *pix* or *fat* and *git* survived to early pupal stages of development, allowing assessment of organ size in larvae. We observed a striking increase in the size of imaginal tissues from *fat, git* compared to *fat* alone, which was especially obvious in leg discs at day 11 (Figures 2J–2L). We performed similar analyses on *fat* and *pix* single- and double-mutant wing discs dissected from tightly developmentally staged animals. Z sections of nonflattened tissues were captured by confocal microscopy, and the volume of each disc was quantified (Figures 2M–2S). At day 6, *pix* mutant wing imaginal discs displayed no obvious increase in volume compared to wild-type wing discs. At day 9 *fat, pix* discs were significantly larger than *fat* discs (Figure 2S). Because control, *pix*, and *git* animals pupate at day 6, we were unable to quantify these tissues at days 9 or 11. In this experiment, *fat* animals pupated before day 11, whereas *fat, pix* mutant animals did not, and contained even larger wing discs (Figure 2S). Together, these data support the idea that both Pix and Git restrict tissue growth and do so in parallel to the Fat branch of the Hippo pathway.

Pix and Git Control Cell Number through Hippo

Pix and Git are known to function together as a scaffold complex to activate the sterile 20-like kinase PAK [32], which is

(F and F′) *D. melanogaster* third-instar larval wing imaginal disc of the genotype *ex-lacZ, en-Gal4, UAS-GFP*; *UAS-Pix RNAi*. Transcriptional activity of the *ex* gene was reported by β-galactosidase expression (grayscale) and in (E′) GFP (green) demarcates the posterior compartment, where Pix RNAi was expressed.
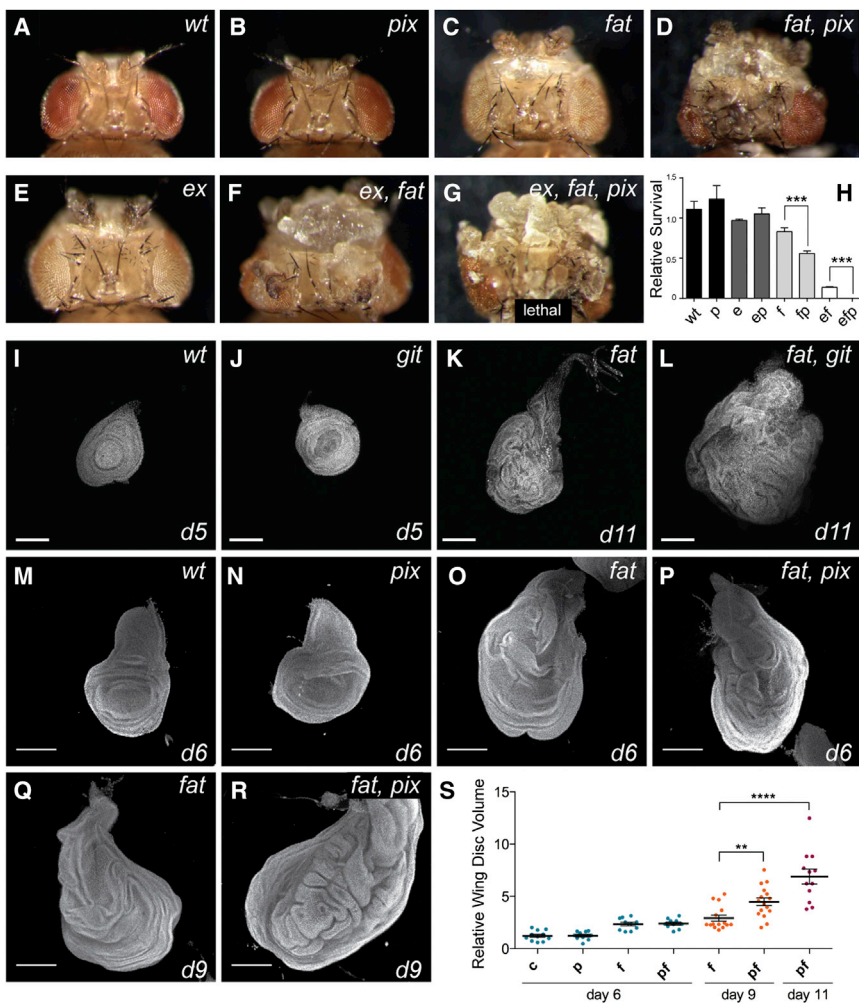
See also Figure S1.

Figure 2. Pix and Git Limit Tissue Growth in Parallel to Fat Cadherin

(A–G) Adult female *D. melanogaster* with head and eye tissue containing homozygous clones generated with *eyeless-Flp* of the following genotypes: wild-type (A), *pix1036* (B), *fatfd* (C), *fatfd, pix1036* (D), *exe1* (E), *exe1, fatfd* (F), and *exe1, fatfd, pix1036* (G).

(H) Relative survival of the genotypes in (A)–(G) was determined by comparison of the number of mutant progeny with the number of their wild-type siblings recovered from crosses. Genotypes of clonal tissue are as follows: wt, wild-type; P, *pix1036*; E, *exe1*; and F, *fatfd*. At least 400 mutant or wild-type siblings were counted per genotype. Data represent the mean ± SEM. ***p < 0.001.

(I–R) Representative final size and age of third instar leg (I–L) and wing (M–R) imaginal discs for the indicated genotypes. Discs were stained with DAPI to mark nuclei. Scale bars, 150 μM.

(S) Quantification of wing disc volume of the indicated genotypes. C, control; f, *fat*; p, *pix*; fp, *fat, pix*. n = 11, 10, 10, 10, 15, 16, and 5 from left to right. Data represent the mean ± SEM. ****p < 0.0001, **p < 0.01.

See also Figure S2.

that Pix and Git regulate cell number and eye growth by acting through Hpo (Figures 3F–3H).

Pix and Git Function as a Bipartite Scaffold to Promote Hippo Dimerization and Activity

Pix and Git perform many of their signal transduction functions by acting as a heterodimeric scaffold [34–37]. To test whether Pix and Git serve as a scaffold

structurally related to Hpo. Given that we identified Pix and Git as Hpo-binding proteins, we investigated the possibility that these three proteins operate together to regulate tissue growth by analyzing genetic interactions with *hpo*. We performed these experiments in pupal eyes, which offer an excellent setting to quantify increases in cell number when tissue growth is deregulated. We used the *eyeless-FLP* system to generate eyes with clones of tissue containing a hypomorphic allele of *hpo* (*hpoMGH1*). As reported previously, *hpoMGH1* mutant eyes displayed an increase in the number of interommatidial cells compared to wild-type eyes (Figures 3A, 3B, and 3H) [9]. We found that combining the *hpoMGH1* allele with mutations in either *git* or *pix* further increased interommatidial cell number (Figures 3C, 3D, and 3H). To test whether Pix and Git act separately or together to regulate the Hippo pathway, we analyzed eye tissue that was triple mutant for *pix*, *git*, and *hpo*. Triple-mutant tissue showed no further increase in interommatidial cell number than did either double mutant, suggesting that Pix and Git act in partnership to regulate the Hippo pathway (Figures 3E and 3H).

To test whether Pix and Git regulate interommatidial cell number through Hpo or in parallel, we also examined their ability to affect cell number in tissue harboring a null allele of *hpo* (*hpo5.1*) that lacks almost the entire Hpo coding sequence [33]. In the background of *hpo* nullizygous tissue, loss of *pix* and *git* no longer affected interommatidial cell number, suggesting

to activate Hpo, we used a series of genetic and biochemical experiments. Hippo pathway hyperactivation retards the growth of tissues such as the eye and wing [9–12, 38]. To determine whether Pix and Git could enhance Hpo's ability to retard tissue growth, we used *D. melanogaster* strains harboring *pix* and *git* transgenes. Pix and Git overexpression did not obviously affect wing or eye size when expressed using the *nub-gal4* and *GMR-Gal4* drivers, respectively, compared to controls (Figures 3I, 3J, and 3N–3P). However, when we doubled the dosage of both *pix* and *git* transgenes, we observed a significant reduction in wing size, consistent with a role for Pix and Git in suppression of organ growth (Figure S3). Overexpression of a weak *hpo* transgene [39] reduced wing size to 60% of control wings but had no obvious effect on eye size or roughness (Figures 3K, 3N, and 3Q). Individual expression of either Pix or Git with Hpo did not enhance Hpo's ability to repress wing size (Figure 3N). However, when Pix, Git, and Hpo were expressed together, a striking decrease in wing size was observed to only 15% the size of wild-type wings (Figures 3L and 3N). Consistently, coexpression of Pix, Git, and Hpo in the eye substantially reduced eye size and increased roughness compared to Hpo overexpression alone (Figures 3Q and 3R). In both eyes and wings, the observed enhancement of Hpo-driven inhibition of tissue growth by Pix and Git was greater than that of simply doubling the dose of the *hpo* transgene (Figures 3M, 3N, and 3S). The
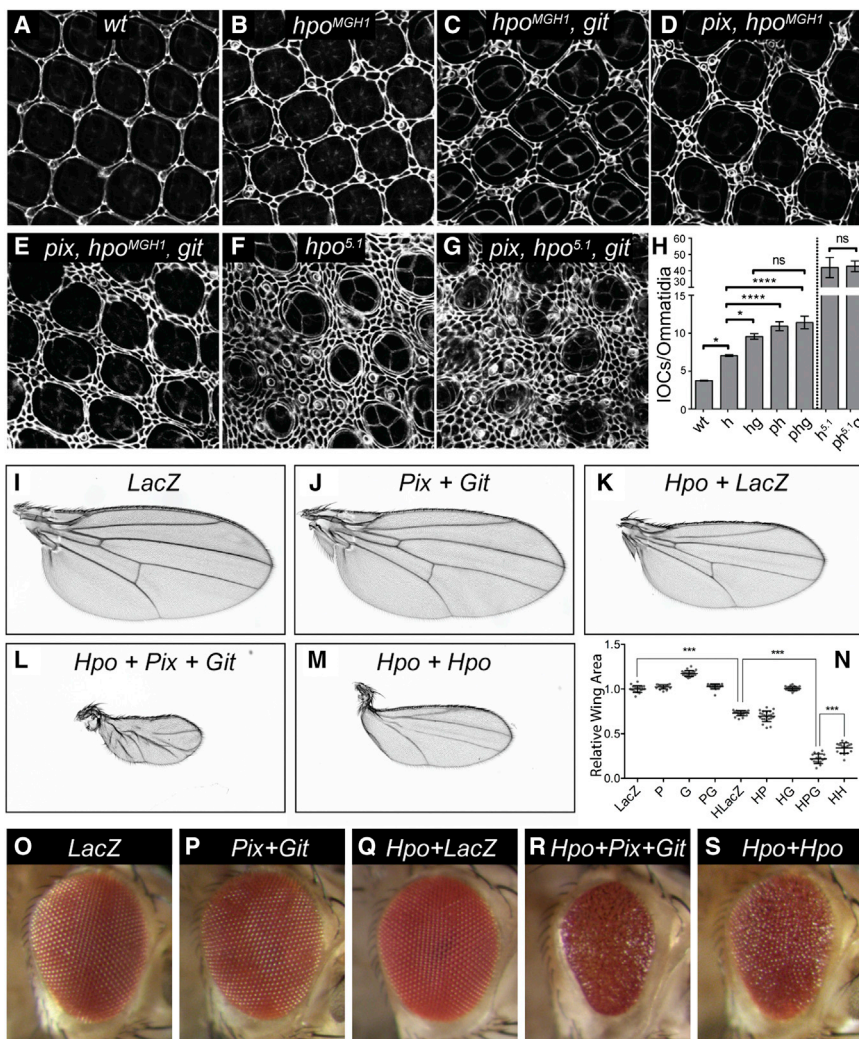
Figure 3. Pix and Git Control Cell Number and Organ Size through Hippo

(A–G) *D. melanogaster* eyes (either wild-type or harboring the indicated mutations) 44 hr after puparium formation, stained with anti-Discs large.

(H) Quantification of interommatidial cell numbers of the genotypes displayed in (A)–(G). n = 5 in (A), n = 8 in (B), n = 10 in (C), n = 12 in (D), n = 9 in (E), n = 3 in (F), and n = 3 in (G). Data represent the mean ± SEM. *p < 0.05, ****p < 0.0001.

(I–S) Adult female *D. melanogaster* wings (I–M) and eyes (O–S) expressing the following transgenes under the control of *nub-Gal4* (I–M) or *GMR-Gal4* (O–S): *UAS-lacZ* (I and O), *UAS-pix, UAS-git* (J and P), *UAS-hpo, UAS-LacZ* (K and Q) *UAS-hpo, UAS-pix, UAS-git* (L and R), and *UAS-hpo/UAS-hpo* (M and S).

(N) Quantification of wing area of the indicated genotypes. n = 19 in (I), n = 22 in (J), n = 21 in (K), n = 16 in (L), and n = 17 in (M). Data represent the mean ± SEM. ***p < 0.001.

See also Figure S3.

observed a more than 3-fold increase in Venus fluorescence, indicative of strong induction of Hpo dimerization (Figures 4B and 4C). This effect was specific to Hpo dimerization, as Pix and Git overexpression failed to influence dimerization of the control proteins Fos and Jun (Figures 4C). Pix and Git overexpression also induced strong association of Hpo with Sav (Figure 4C), suggesting that Pix and Git influence Hpo's ability to engage with and activate the Hippo pathway core kinase cassette, which is consistent with our findings that Pix and Git influence Yki activity and enhance Hpo's ability to retard organ growth.

observed requirement for both Pix and Git to be overexpressed simultaneously in order to enhance Hpo-driven growth retardation is consistent with the idea that Pix and Git function together in a complex to activate Hpo. The observation that Pix and Git overexpression minimally influence organ size but enhance Hpo's ability to limit organ size is reminiscent of experiments with Sav, which serves as a scaffold for Hpo and Wts; *GMR-Gal4*-dependent Sav expression has no phenotype, but it enhances the ability of both Hpo and Wts to limit eye size [12, 38].

Hpo and its mammalian orthologs are known to dimerize and this is essential for kinase activation [39–41]. Based on our findings above, we predicted that Pix and Git would promote Hpo dimerization. To test this, we employed transgenic *D. melanogaster* strains expressing split Venus-tagged Hpo kinase-dead proteins HpoVC and HpoVN (wild-type Hpo was unsuitable as it caused substantial reduction of wing imaginal disc tissue when driven with *nub-Gal4*). In this system, Venus fluorescence is only detectable when Hpo dimerizes, and in doing so brings the N- and C-terminal halves of Venus together [39]. In control wing imaginal discs expressing HpoVC and HpoVN alone, as well as in discs additionally expressing either Pix or Git, we observed very low Venus fluorescence (Figures 4A and 4C). When Pix and Git were expressed together, we

To test biochemically whether Pix and Git activate Hpo, we assessed their ability to regulate phosphorylation of the Hpo activation loop (threonine 195), a well-characterized marker of activity of Hpo and its mammalian orthologs MST1 and MST2 [42, 43]. Overexpression of either Pix or Git alone in *D. melanogaster* S2 cells had no significant impact on Hpo activity, whereas Pix and Git cooverexpression resulted in an approximate doubling of Hpo T195 phosphorylation compared to Hpo alone (Figures 4D and S4F).

Pix and Git Act as a Scaffold, Rather than Enzymes, to Activate Hippo
Given that Pix and Git promoted Hpo dimerization, we considered that they might activate Hpo by promoting Hpo transphosphorylation, a key mechanism of Hpo and MST1/MST2 activation in *D. melanogaster* and mammals, respectively [39, 41–43]. Alternatively, Pix and Git could modulate the activity of other kinases that are known to phosphorylate the activation loop of Hpo, such as Tao-1 [13, 14]. To distinguish between these two scenarios, we expressed either wild-type or kinase dead (carrying a mutation in the ATP-binding site, K71R) versions of Hpo in the presence and absence of both Pix and Git and assessed Hpo-T195 phosphorylation. Pix and Git only enhanced Hpo activation loop phosphorylation
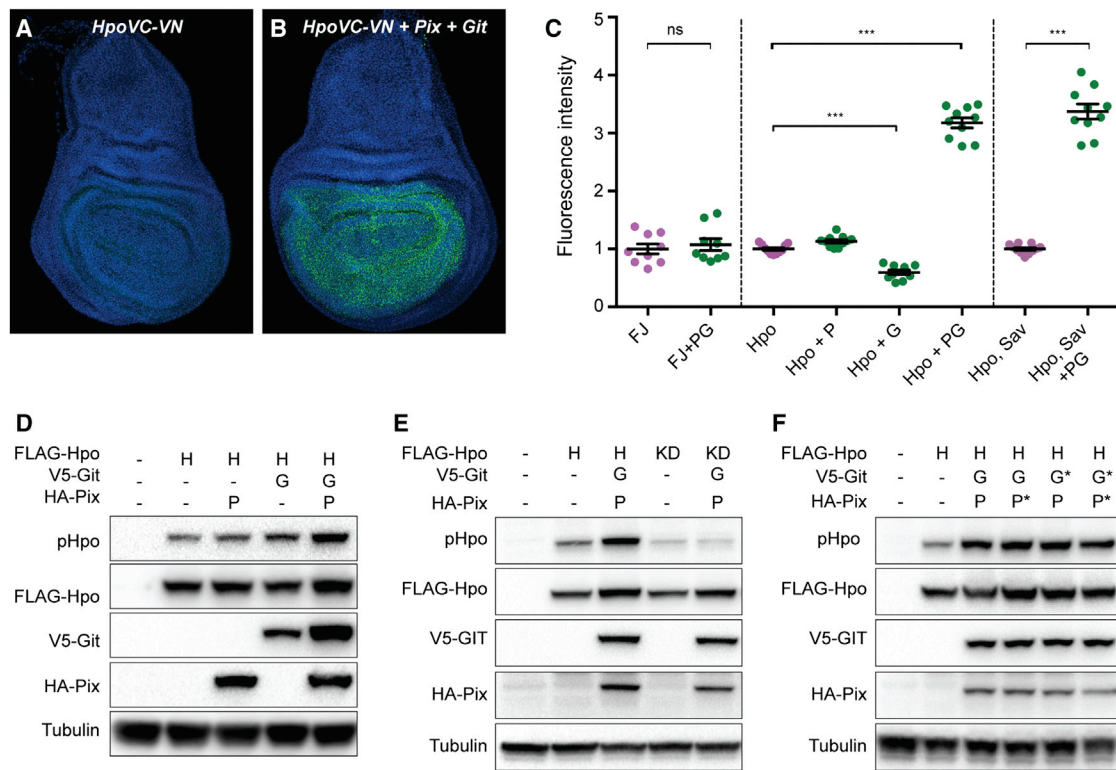
Figure 4. Pix and Git Function as a Bipartite Scaffold to Dimerize and Activate Hippo

(A and B) Third-instar larval wing imaginal discs stained with DAPI (blue). Both tissues express Hpo kinase-dead proteins fused to either the N or C terminus of Venus fluorescent protein (green). The tissue in (B) also expresses Pix and Git.

(C) Quantification of Venus fluorescence in larval wing imaginal discs of the indicated genotypes (F, Fos; J, Jun; P, Pix; G, Git). n = 9, 9, 11, 11, 10, 10, 11, and 10 from left to right. Data represent the mean ± SEM. ***p < 0.001. ns, no significant difference.

(D–F) Western blot analysis of protein lysates from S2 cells transfected with the indicated plasmids. Hpo phosphorylation was detected using an antibody recognizing phosphorylation of the Hpo activation loop (T195). Western blots were also probed with anti-Flag, anti-HA, anti-V5, and anti-tubulin to reveal total Hpo, Pix, Git, and tubulin respectively.

See also Figure S4.

when coexpressed with active Hpo, suggesting that Pix and Git potentiate Hpo transphosphorylation rather than phosphorylation by additional regulatory proteins (Figure 4E).

Next, we more formally addressed whether Pix and Git act as scaffolds to activate Hpo as these proteins have been reported to function as both enzymes and scaffolds. For example, Pix enzymatic activity is required to activate the Rho-GTPases Rac1 and Cdc42, whereas Git enzymatic activity is required to deactivate ARF family GTPases. To discern between these possibilities, we generated mutant versions of Pix and Git that are known to abolish their enzymatic activity; Pix serine 89 was mutated to glutamic acid (S89E) [44], and Git arginine 39 was mutated to lysine (R39K) [32]. We then coexpressed wild-type or enzymatic-dead (denoted by *) Pix and Git in the indicated combinations with Hpo (Figure 4F). In each scenario, Pix and Git overexpression was still able to robustly promote Hpo activation, as assessed by Hpo-T195 phosphorylation (Figure 4F). Given that in mammalian cultured cells, Pix and Git activate PAK [32] and that PAK was recently linked to Hippo signaling [45], we considered the possibility that Pix and Git activate Hpo via the *Drosophila* homologs of PAK (Pak1 and Pak3), but we found no evidence for this (Figure S4). Together, these data indicate that Pix and Git activate Hpo by acting as scaffolds rather than enzymes, an assertion that is further supported by our gain-of-function data in cultured cells and in vivo, where overexpression of both Pix

and Git were required to activate Hpo and enhance its ability to retard tissue growth. Pix and Git might enhance local concentrations of Hpo within cells to enable Hpo activation and/or facilitate structural changes that promote transphosphorylation between Hpo dimers. Such studies will be most informative in tissues that the Hippo pathway is known to control the growth of, such as imaginal discs.

Conclusions

Most founding members of the Hippo pathway were identified in clonal homozygous screens. The present study highlights the importance of more recent biochemical and RNAi approaches that have identified Hippo pathway genes that were not recovered using other methods. Further, this study underscores the high level of redundancy inherent in upstream regulators of the Hippo pathway, as growth regulatory roles for Pix and Git were only revealed when they were disabled in the context of mutations in the Fat upstream branch of the Hippo pathway. The Hippo pathway is known to regulate the growth of many tissues in addition to imaginal discs, and upstream regulators of the Hippo pathway show varying degrees of redundancy in these tissues [2, 4, 23]. Therefore, it is conceivable that Pix and Git regulate Hippo pathway activity in a nonredundant fashion in non-imaginal-disc tissues. Currently, it is unclear what controls Pix and Git in their ability to regulate Hpo. One possibility is that Pix and Git provide a link

between the apicobasal polarity protein Scribble and the Hippo pathway. Scribble has been linked to Pix and Git in mammalian cells [35] and has been shown to affect Hippo pathway activity in both *D. melanogaster* and in mammalian cells [2, 4, 23]. A further intriguing possibility is that Pix and Git provide a connection between integrins, focal adhesions, and Hippo signaling. Pix and Git are known to regulate focal adhesion turnover, and they localize at focal adhesions through Git's ability to bind to Paxillin. Pix and Git are also well-known mediators of mechanical information [46]. Therefore, in the context of tissue growth control, Pix and Git could conceivably provide a biochemical link between mechanical information from integrins and/or focal adhesions to the Hippo pathway core kinase cassette.

Experimental Procedures

D. melanogaster Stocks
Transgenic *D. melanogaster* stocks were generated that harbored the N-terminally tagged *UAS-HA-Pix* and *UAS-MYC-Git* coding sequences on the third chromosome. Other stocks were *UAS-LacZ, UAS-GFP, GMR-Gal4, en-Gal4, nub-Gal4,* y w *eyFlp; FRT42D P[W+ ubi-GFP], UAS-Pix-1 RNAi* (BSC#32974), *ban-lacZ,* and *ex^697* (all Bloomington Stock Center); *pix* (*dpix^1036*) [47]; *git* (*dgit^ex21c*) [48]; and *hpo^MGH1, hpo5.1, ft^422, ft^fd, ex^MGH1, ex^e1, UAS-Dicer, UAS-Yki RNAi* (KK 104523), *UAS-LacZ RNAi* (GD 51446), *UAS-Sd RNAi* (KK 108877), *UAS-Pak1 RNAi* (KK 108937), and *UAS-Pak3 RNAi* (GD 39844) (all Vienna *Drosophila* RNAi Center). All *D. melanogaster* expressing transgenic constructs were reared at 25°C, with the exception of animals in Figures 3O–3S, which were raised at 18°C.

Immunofluorescence
Primary antibodies were specific for β-galactosidase (Sigma), Discs large, and Cubitus interruptus (both Developmental Studies Hybridoma Bank). Anti-mouse secondary antibodies were from Invitrogen. Tissues were stained as in [21]. DAPI was used to visualize nuclei in third-instar wing and leg imaginal discs.

Quantification of Organ Size
Wings were dissected from adult female flies reared at 25°C and were mounted in Canada Balsam (Sigma). Wing sizes were quantified using Adobe Photoshop as in [21]. The mean and SEM values of wing area were determined with GraphPad Prism. Flies laid eggs for 4 hr, and wing imaginal discs were dissected from developmentally staged animals and stained with DAPI. Z sections of nonflattened tissues were captured using a confocal microscope, and Imaris software was used to quantify the volume of each disc. For statistical analysis, genotypes were compared using an ANOVA test, followed by a post hoc Tukey's test to determine which genotypes were different from one another. When only two genotypes were compared, a Student's t test was used. p values <0.05 were considered significant.

Quantification of Relative Survival
FRT males that were heterozygous for a mutation of interest were mated to *eyeless-FLP* females. This mating is expected to produce F1 progeny that contain either wild-type or mutant clones at a 1:1 ratio. The ratio of wild-type and mutant F1 progeny was recorded for each genotype and compared. For statistical analysis, genotypes were compared using unpaired Student's t tests. p values <0.05 were considered significant.

Expression Plasmids
A complete Hpo open reading frame was cloned into pMK33-NTAP-GS or pMK33-CTAP-SG vectors [17] to generate N- or C-terminally tagged Hpo, respectively. *D. melanogaster pix* and *git* coding sequences in the pXJ40 plasmid were gifts from E. Manser. To constitutively express these genes in cell culture, we subcloned N-terminally tagged HA-pix and V5-git sequences into the pAc5.1 vector. To generate transgenic *D. melanogaster*, we cloned N-terminally tagged HA-Pix and MYC-Git coding sequences into the pUAST vector. In order to express Pix protein without GEF enzymatic activity, we performed site-directed mutagenesis to change serine 89 to glutamic acid (S89E) [44]. To express Git protein without GAP enzymatic activity, we used site-directed mutagenesis to change arginine 39 to lysine (R39K) [32]. pAc5.1-Hpo, pAc5.1-Hpo K71R, and pAc5.1-RASSF were from N. Tapon [11, 15].

Affinity Purification and Mass Spectrometry
pMK33-TAP-GS Hpo plasmid constructs were used to establish stable S2 cell lines using hygromycin selection. Cells were induced with CuSO$_4$, and protein extracts were prepared as in [17]. Extracts were incubated with streptavidin beads (Pierce) and washed with lysis buffer, and proteins were eluted with 2 mM biotin in lysis buffer, precipitated with TCA, and separated on a short SDS-PAGE. Gel slices were submitted for mass-spectrometry analysis and protein identification, which were performed at the Taplin Mass Spectrometry Facility at Harvard Medical School. Lists of identified proteins were statistically analyzed against six independent control samples from untransfected S2 cells using the SAINT program [18].

Immunoblotting
S2 cells were transfected with the indicated plasmids and lysed after 48 hr, whereas third-instar larval imaginal discs were dissected and lysed directly. Lysates were immunoprecipitated or directly subjected to SDS-PAGE and transferred to PVDF (Millipore). Membranes were immunoblotted with antibodies specific for HA tag (Invitrogen), Flag tag (Sigma), V5 tag (Invitrogen), GFP (Roche), phospho-T195-Hpo (Cell Signaling), or Tubulin (Sigma).

Supplemental Information

Supplemental Information includes four figures and one table and can be found with this article online at http://dx.doi.org/10.1016/j.cub.2014.11.041.

References

1. Harvey, K.F., Zhang, X., and Thomas, D.M. (2013). The Hippo pathway and human cancer. Nat. Rev. Cancer *13*, 246–257.
2. Schroeder, M.C., and Halder, G. (2012). Regulation of the Hippo pathway by cell architecture and mechanical signals. Semin. Cell Dev. Biol. *23*, 803–811.
3. Yu, F.X., and Guan, K.L. (2013). The Hippo pathway: regulators and regulations. Genes Dev. *27*, 355–371.
4. Genevet, A., and Tapon, N. (2011). The Hippo pathway and apico-basal cell polarity. Biochem. J. *436*, 213–224.
5. Premont, R.T., Claing, A., Vitale, N., Freeman, J.L., Pitcher, J.A., Patton, W.A., Moss, J., Vaughan, M., and Lefkowitz, R.J. (1998). beta2-Adrenergic receptor regulation by GIT1, a G protein-coupled receptor kinase-associated ADP ribosylation factor GTPase-activating protein. Proc. Natl. Acad. Sci. USA *95*, 14082–14087.
6. Manser, E., Loo, T.H., Koh, C.G., Zhao, Z.S., Chen, X.Q., Tan, L., Tan, I., Leung, T., and Lim, L. (1998). PAK kinases are directly coupled to the PIX family of nucleotide exchange factors. Mol. Cell *1*, 183–192.
7. Feng, Q., Albeck, J.G., Cerione, R.A., and Yang, W. (2002). Regulation of the Cool/Pix proteins: key binding partners of the Cdc42/Rac targets, the p21-activated kinases. J. Biol. Chem. *277*, 5644–5650.
8. Feng, Q., Baird, D., and Cerione, R.A. (2004). Novel regulatory mechanisms for the Dbl family guanine nucleotide exchange factor Cool-2/alpha-Pix. EMBO J. *23*, 3492–3504.

9. Harvey, K.F., Pfleger, C.M., and Hariharan, I.K. (2003). The Drosophila Mst ortholog, hippo, restricts growth and cell proliferation and promotes apoptosis. Cell *114*, 457–467.

10. Udan, R.S., Kango-Singh, M., Nolo, R., Tao, C., and Halder, G. (2003). Hippo promotes proliferation arrest and apoptosis in the Salvador/Warts pathway. Nat. Cell Biol. *5*, 914–920.

11. Pantalacci, S., Tapon, N., and Léopold, P. (2003). The Salvador partner Hippo promotes apoptosis and cell-cycle exit in Drosophila. Nat. Cell Biol. *5*, 921–927.

12. Wu, S., Huang, J., Dong, J., and Pan, D. (2003). hippo encodes a Ste-20 family protein kinase that restricts cell proliferation and promotes apoptosis in conjunction with salvador and warts. Cell *114*, 445–456.

13. Poon, C.L., Lin, J.I., Zhang, X., and Harvey, K.F. (2011). The sterile 20-like kinase Tao-1 controls tissue growth by regulating the Salvador-Warts-Hippo pathway. Dev. Cell *21*, 896–906.

14. Boggiano, J.C., Vanderzalm, P.J., and Fehon, R.G. (2011). Tao-1 phosphorylates Hippo/MST kinases to regulate the Hippo-Salvador-Warts tumor suppressor pathway. Dev. Cell *21*, 888–895.

15. Polesello, C., Huelsmann, S., Brown, N.H., and Tapon, N. (2006). The Drosophila RASSF homolog antagonizes the hippo pathway. Curr. Biol. *16*, 2459–2465.

16. Ribeiro, P.S., Josué, F., Wepf, A., Wehr, M.C., Rinner, O., Kelly, G., Tapon, N., and Gstaiger, M. (2010). Combined functional genomic and proteomic approaches identify a PP2A complex as a negative regulator of Hippo signaling. Mol. Cell *39*, 521–534.

17. Kyriakakis, P., Tipping, M., Abed, L., and Veraksa, A. (2008). Tandem affinity purification in Drosophila: the advantages of the GS-TAP system. Fly (Austin) *2*, 229–235.

18. Choi, H., Larsen, B., Lin, Z.Y., Breitkreutz, A., Mellacheruvu, D., Fermin, D., Qin, Z.S., Tyers, M., Gingras, A.C., and Nesvizhskii, A.I. (2011). SAINT: probabilistic scoring of affinity purification-mass spectrometry data. Nat. Methods *8*, 70–73.

19. Poon, C.L., Zhang, X., Lin, J.I., Manning, S.A., and Harvey, K.F. (2012). Homeodomain-interacting protein kinase regulates Hippo pathway-dependent tissue growth. Curr. Biol. *22*, 1587–1594.

20. Hamaratoglu, F., Willecke, M., Kango-Singh, M., Nolo, R., Hyun, E., Tao, C., Jafar-Nejad, H., and Halder, G. (2006). The tumour-suppressor genes NF2/Merlin and Expanded act through Hippo signalling to regulate cell proliferation and apoptosis. Nat. Cell Biol. *8*, 27–36.

21. Degoutin, J.L., Milton, C.C., Yu, E., Tipping, M., Bosveld, F., Yang, L., Bellaiche, Y., Veraksa, A., and Harvey, K.F. (2013). Riquiqui and mini-brain are regulators of the hippo pathway downstream of Dachsous. Nat. Cell Biol. *15*, 1176–1185.

22. Herranz, H., Hong, X., and Cohen, S.M. (2012). Mutual repression by bantam miRNA and Capicua links the EGFR/MAPK and Hippo pathways in growth control. Curr. Biol. *22*, 651–657.

23. Grusche, F.A., Richardson, H.E., and Harvey, K.F. (2010). Upstream regulation of the hippo size control pathway. Curr. Biol. *20*, R574–R582.

24. Baumgartner, R., Poernbacher, I., Buser, N., Hafen, E., and Stocker, H. (2010). The WW domain protein Kibra acts upstream of Hippo in Drosophila. Dev. Cell *18*, 309–316.

25. Genevet, A., Wehr, M.C., Brain, R., Thompson, B.J., and Tapon, N. (2010). Kibra is a regulator of the Salvador/Warts/Hippo signaling network. Dev. Cell *18*, 300–308.

26. Yu, J., Zheng, Y., Dong, J., Klusza, S., Deng, W.M., and Pan, D. (2010). Kibra functions as a tumor suppressor protein that regulates Hippo signaling in conjunction with Merlin and Expanded. Dev. Cell *18*, 288–299.

27. Feng, Y., and Irvine, K.D. (2007). Fat and expanded act in parallel to regulate growth through warts. Proc. Natl. Acad. Sci. USA *104*, 20362–20367.

28. Bennett, F.C., and Harvey, K.F. (2006). Fat cadherin modulates organ size in Drosophila via the Salvador/Warts/Hippo signaling pathway. Curr. Biol. *16*, 2101–2110.

29. Willecke, M., Hamaratoglu, F., Kango-Singh, M., Udan, R., Chen, C.L., Tao, C., Zhang, X., and Halder, G. (2006). The fat cadherin acts through the hippo tumor-suppressor pathway to regulate tissue size. Curr. Biol. *16*, 2090–2100.

30. Silva, E., Tsatskis, Y., Gardano, L., Tapon, N., and McNeill, H. (2006). The tumor-suppressor gene fat controls tissue growth upstream of expanded in the hippo signaling pathway. Curr. Biol. *16*, 2081–2089.

31. Cho, E., Feng, Y., Rauskolb, C., Maitra, S., Fehon, R., and Irvine, K.D. (2006). Delineation of a Fat tumor suppressor pathway. Nat. Genet. *38*, 1142–1150.

32. Loo, T.H., Ng, Y.W., Lim, L., and Manser, E. (2004). GIT1 activates p21-activated kinase through a mechanism independent of p21 binding. Mol. Cell. Biol. *24*, 3849–3859.

33. Genevet, A., Polesello, C., Blight, K., Robertson, F., Collinson, L.M., Pichaud, F., and Tapon, N. (2009). The Hippo pathway regulates apical-domain size independently of its growth-control function. J. Cell Sci. *122*, 2360–2370.

34. Premont, R.T., Perry, S.J., Schmalzigaug, R., Roseman, J.T., Xing, Y., and Claing, A. (2004). The GIT/PIX complex: an oligomeric assembly of GIT family ARF GTPase-activating proteins and PIX family Rac1/Cdc42 guanine nucleotide exchange factors. Cell. Signal. *16*, 1001–1011.

35. Audebert, S., Navarro, C., Nourry, C., Chasserot-Golaz, S., Lécine, P., Bellaiche, Y., Dupont, J.L., Premont, R.T., Sempéré, C., Strub, J.M., et al. (2004). Mammalian Scribble forms a tight complex with the betaPIX exchange factor. Curr. Biol. *14*, 987–995.

36. Zhao, Z.S., Manser, E., Loo, T.H., and Lim, L. (2000). Coupling of PAK-interacting exchange factor PIX to GIT1 promotes focal complex disassembly. Mol. Cell. Biol. *20*, 6354–6363.

37. Frank, S.R., and Hansen, S.H. (2008). The PIX-GIT complex: a G protein signaling cassette in control of cell shape. Semin. Cell Dev. Biol. *19*, 234–244.

38. Tapon, N., Harvey, K.F., Bell, D.W., Wahrer, D.C., Schiripo, T.A., Haber, D., and Hariharan, I.K. (2002). salvador Promotes both cell cycle exit and apoptosis in Drosophila and is mutated in human cancer cell lines. Cell *110*, 467–478.

39. Deng, Y., Matsui, Y., Zhang, Y., and Lai, Z.C. (2013). Hippo activation through homodimerization and membrane association for growth inhibition and organ size control. Dev. Biol. *375*, 152–159.

40. Creasy, C.L., Ambrose, D.M., and Chernoff, J. (1996). The Ste20-like protein kinase, Mst1, dimerizes and contains an inhibitory domain. J. Biol. Chem. *271*, 21049–21053.

41. Jin, Y., Dong, L., Lu, Y., Wu, W., Hao, Q., Zhou, Z., Jiang, J., Zhao, Y., and Zhang, L. (2012). Dimerization and cytoplasmic localization regulate Hippo kinase signaling activity in organ size control. J. Biol. Chem. *287*, 5784–5796.

42. Deng, Y., Pang, A., and Wang, J.H. (2003). Regulation of mammalian STE20-like kinase 2 (MST2) by protein phosphorylation/dephosphorylation and proteolysis. J. Biol. Chem. *278*, 11760–11767.

43. Glantschnig, H., Rodan, G.A., and Reszka, A.A. (2002). Mapping of MST1 kinase sites of phosphorylation. Activation and autophosphorylation. J. Biol. Chem. *277*, 42987–42996.

44. Aghazadeh, B., Zhu, K., Kubiseski, T.J., Liu, G.A., Pawson, T., Zheng, Y., and Rosen, M.K. (1998). Structure and mutagenesis of the Dbl homology domain. Nat. Struct. Biol. *5*, 1098–1107.

45. Nguyen, H.T., Hong, X., Tan, S., Chen, Q., Chan, L., Fivaz, M., Cohen, S.M., and Voorhoeve, P.M. (2014). Viral small T oncoproteins transform cells by alleviating hippo-pathway-mediated inhibition of the YAP proto-oncogene. Cell Rep. *8*, 707–713.

46. Zhang, H., Landmann, F., Zahreddine, H., Rodriguez, D., Koch, M., and Labouesse, M. (2011). A tension-induced mechanotransduction pathway promotes epithelial morphogenesis. Nature *471*, 99–103.

47. Parnas, D., Haghighi, A.P., Fetter, R.D., Kim, S.W., and Goodman, C.S. (2001). Regulation of postsynaptic structure and protein localization by the Rho-type guanine nucleotide exchange factor dPix. Neuron *32*, 415–424.

48. Bahri, S.M., Choy, J.M., Manser, E., Lim, L., and Yang, X. (2009). The Drosophila homologue of Arf-GAP GIT1, dGIT, is required for proper muscle morphogenesis and guidance during embryogenesis. Dev. Biol. *325*, 15–23.